Heliyon 8 (2022) e09943

Contents lists available at ScienceDirect

Heliyon

journal homepage: www.cell.com/heliyon

Research article

Anion-assisted supramolecular assemblies of zinc(II) complexes with isonicotinamide☆

Željka Soldin [a,*], Boris-Marko Kukovec [b,**], Tamara Debač [c,d], Marijana Đaković [a], Zora Popović [a]

[a] Division of General and Inorganic Chemistry, Department of Chemistry, Faculty of Science, University of Zagreb, Horvatovac 102a, HR-10000 Zagreb, Croatia
[b] Department of Physical Chemistry, Faculty of Chemistry and Technology, University of Split, Ruđera Boškovića 35, HR-21000 Split, Croatia
[c] Elementary School Ferdinandovac, Dravska 66, HR-48356 Ferdinandovac, Croatia
[d] Elementary School Đurđevac, Ulica Đure Basariček a 5D, HR-48350 Đurđevac, Croatia

GRAPHICAL ABSTRACT

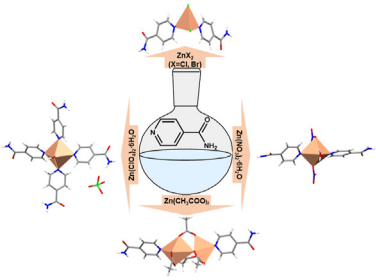

ARTICLE INFO

Keywords:
Anion-assisted assembly
Coordination polyhedron
Isonicotinamide
Zinc(II)
Amide-amide homosynthon

ABSTRACT

Five zinc(II) coordination compounds, $[ZnCl_2(isn)_2]$ (**1**), $[ZnBr_2(isn)_2]$ (**2**), $[Zn(NO_3)_2(H_2O)(isn)_2]$ (**3**), $[Zn(CH_3COO)_2(isn)]_2$ (**4**) and $[Zn(isn)_4(H_2O)_2](ClO_4)_2$ (**5**) (isn = isonicotinamide), were prepared by the reactions of the isonicotinamide (pyridine-4-carboxamide, isn) and corresponding zinc(II) salts. Their crystal structures were determined by the single-crystal X-ray diffraction method. The coordination environment of zinc(II) is tetrahedral in the compounds containing small halide anions (chloride, bromide), **1** and **2**. An expansion of the zinc(II) coordination environment to the octahedral is observed in the presence of the monodentate and bridging nitrate ions in **3**. The coordination environments of both zinc(II) ions in dimeric acetate complex **4** is also enlarged in the comparison with **1** and **2**, one zinc(II) ion being octahedrally coordinated and the other being pentacoordinated. The zinc(II) ion in **5** also reaches higher coordination environment (octahedral), which is enabled by binding of additional water molecules, since the perchlorate ion is uncoordinated. The supramolecular amide-amide homosynthon $R_2^2(8)$ is preserved in the presence of halide, nitrate and acetate ions (**1**–**4**), but it is completely disrupted in the crystal packing of **5** due to the presence of the bulky perchlorate anion. Spectroscopic analysis of compounds **1**–**5** was performed by IR spectroscopy in the solid state and by ^{13}C NMR spectroscopy in the DMSO solutions. The NMR data support a complete decomposition of **3** in the DMSO solution, but **1**, **2**, **4** and **5** remain unchanged in the solution. Thermal properties of the coordination compounds were also investigated by TGA and DSC methods.

☆ This article is a part of the "Coordination compounds" Special issue.

* Corresponding author.
** Corresponding author.
E-mail addresses: zeljka@chem.pmf.hr (Ž. Soldin), bmkukovec@ktf-split.hr (B.-M. Kukovec).

https://doi.org/10.1016/j.heliyon.2022.e09943
Received 21 March 2022; Received in revised form 6 May 2022; Accepted 8 July 2022

1. Introduction

An employment of pyridine-amide based ligands equipped with a pyridyl donor group and a pronounced hydrogen bonding functionality (amide group) may lead to the formation of different supramolecular structures. Introduction of a metal center enables formation of more diverse coordinations and topologies [1, 2, 3, 4, 5, 6, 7, 8, 9, 10]. The dual ability of a self-assembly through formation of covalent bonds to a metal center, together with establishing robust and well-known supramolecular synthons via hydrogen bonding, can be therefore used as a powerful crystal engineering tool [11, 12, 13, 14]. Coordination compounds with such ligands can be used in various areas as materials with improved catalytic, adsorption, conductive, biomedical, electronical, optical or magnetic properties [2, 5, 6, 11, 15, 16, 17]. Variety of possible applications makes the design of new metal-organic structures, linked by noncovalent interactions, to be one of the topic interests in materials science. Reactivity and physical properties of the solids are closely related to the manner in which building units are linked together in the crystal structure, which enables a fine tuning of desired material property by impacting on the crystal structure. This can be achieved by changing some key parameters like coordination geometry of the metal ion, type of the counter-ion, selection of solvent, metal-to-ligand ratio, temperature etc. [9, 15, 18, 19, 20, 21, 22, 23, 24].

Transition metal ions are usually capable of displaying a range of different coordination geometries which can be controlled in order to obtain the desired supramolecular assembly. The coordination environment of zinc(II) is quite unpredictable and can vary from tetrahedral, pentacoordinated to octahedral, neither being more stable than the other. The main reason is the absence of the crystal field splitting stabilization, as zinc(II) 3*d* orbitals are completely filled [25]. Therefore, the zinc(II) coordination environment is primarily influenced by zinc(II) radius and by the availability of the donor atoms that can coordinate zinc(II). First of our goals was to tune the zinc(II) coordination environment by selecting anions with different coordination ability – from simple halide anions (chloride, bromide), bulky perchlorate anion to nitrate and acetate anions with multiple O donor atoms with a coordination potential to either chelate or bridge the zinc(II) ions. In the presence of smaller halide ions, zinc(II) is expected to be low-coordinated, but its coordination number is expected to enlarge in the presence of the available O donor atoms from either perchlorate, nitrate or acetate ions.

Our second goal was to study the influence of the introduced anions on the supramolecular features of the prepared zinc(II) coordination compounds with isonicotinamide (pyridine-4-carboxamide, isn), in particular on the persistence or disruption of the centrosymmetric amide-amide supramolecular homosynthon (a $R_2^2(8)$ hydrogen-bonded ring motif, Scheme 1) [13, 26, 27, 28, 29, 30] in the presence of the various anions with a proton-accepting capability.

The isonicotinamide was deliberately used in the design of our zinc(II) coordination compounds since it is a ligand with a predictable coordination mode towards zinc(II) ion – binding to a zinc(II) ion in a monodentate fashion via its pyridine N atom and leaving the amide group uncoordinated and able to participate in the expected supramolecular amide-amide homosynthon $R_2^2(8)$. Our idea was to test the robustness of this common supramolecular homosynthon, that is frequently found in the crystal structures of both organic and metal-organic amide compounds. Therefore, we have introduced various anions (halide ions, perchlorate, nitrate, acetate) that can act as proton acceptors by competing for the amide protons in the respective crystal packings, in order to check whether this amide-amide supramolecular homosynthon $R_2^2(8)$ would be preserved of disrupted and whether there is a pattern for a prediction of such behavior.

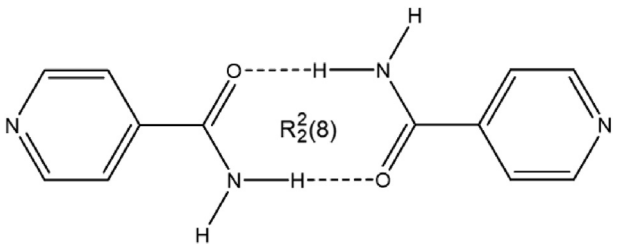

Scheme 1. The amide-amide $R_2^2(8)$ supramolecular synthon.

In order to study the impact of different anions on coordination geometry of the zinc(II) ion and robustness of the amide-amide supramolecular homosynthon, we have prepared and characterized five new zinc(II) coordination compounds, $[ZnCl_2(isn)_2]$ (**1**), $[ZnBr_2(isn)_2]$ (**2**), $[Zn(NO_3)_2(H_2O)(isn)_2]$ (**3**), $[Zn(CH_3COO)_2(isn)]_2$ (**4**) and $[Zn(isn)_4(H_2O)_2](ClO_4)_2$ (**5**).

2. Experimental

2.1. Materials and physical measurements

All commercially available chemicals are of a reagent grade and were used as received without further purification. CHN elemental analyses were carried out with a Perkin-Elmer 2400 Series II CHNS analyzer in the Analytical Services Laboratories of the Ruđer Bošković Institute, Zagreb, Croatia. The zinc content in the complexes was determined by complexometric titration with EDTA (at pH 10 using Eriochrome Black T indicator) of the solution obtained after decomposition of the compounds in hydrochloric acid (2 mol dm^{-3}) [31,32].

IR spectra were obtained in the range 4000–500 cm^{-1} on a Perkin-Elmer Spectrum Two FTIR spectrometer equipped with a universal ATR (single reflection diamond) accessory.

The one-dimensional homonuclear ^{13}C NMR spectra were recorded with a Bruker AV 600 spectrometer, operating at 150.917 MHz. The samples were dissolved in DMSO-d_6 in 5 mm NMR tubes. Chemical shifts, in ppm, are referred to TMS as internal standard.

Thermogravimetric analysis was performed using a simultaneous TGA-DTA analyzer (Mettler-Toledo TGA/SDTA 851e). DSC measurements were performed on the Mettler–Toledo DSC823e calorimeter. The samples were placed in aluminum pans (40 μL), heated in flowing nitrogen (50 mL min^{-1}) from room temperature up to 600 °C (TGA) and 400 °C (DSC) at a rate of 10 °C min^{-1}. Data collection and analysis were performed using the program package STARe Software 16.40 MettlerToledo GmbH.

Powder X-ray diffraction (PXRD) traces were measured on a Malvern Panalytical Aeris XRD diffractometer with CuKα (1.5406 Å) radiation, Ni filter and solid-state PIXcel3D-Medipix3 detector. Samples were prepared as a thin layer on a silicon zero-background plate. Data were collected in the 2θ range from 5° to 50° with a step size of 0.02173°, scan rate 10 s/°, ¼ inch divergence slit and 13 mm beam mask. The Rietveld refinement in 2θ range from 5 to 50° was performed using Topas Academic V5 program package [33].

2.2. Syntheses of the compounds

2.2.1. $[ZnCl_2(isn)_2]$ (1)

A solution of isn (0.54 g, 4.4 mmol) in 15 mL EtOH was added dropwise to a solution of $ZnCl_2$ (0.30 g, 2.2 mmol) in 20 mL EtOH and stirred for 20 min. The colorless crystals were filtered off, washed with EtOH and dried in air. The colorless crystals suitable for single-crystal X-ray structure determination were isolated from mother liquor after a few days. Yield: 88 % (based on $ZnCl_2$). Anal. Calc. for $ZnCl_2C_{12}H_{12}N_4O_2$: C, 37.87; H, 3.18; N, 14.72; Zn, 17.19. Found: C, 37.91; H, 3.24; N, 14.98; Zn, 17.99.

IR (ATR, cm^{-1}): 3431(w), 3386(w), 3319(w), 3264(w), 3158(w), 3048(w), 1711(m), 1678(s), 1619(m), 1598(m), 1556(m), 1422(m), 1394(m), 1331(w), 1236(w), 1221(w), 1152(w), 1123(w), 1086(w),

1061(m), 1031(m), 866(m), 856(m), 799(w), 760(s), 712(m), 652(m), 627(m), 594(s), 518(vs), 447(m).

^{13}C NMR (DMSO-d$_6$, δ/ppm): 150.39 (C-2,6), 122.29 (C-3,5), 142.47 (C-4), 166.58 (C-7).

2.2.2. [$ZnBr_2(isn)_2$] (2)

A solution of isn (0.33 g, 2.6 mmol) in 10 mL EtOH was added dropwise to a solution of $ZnBr_2$ (0.30 g, 1.3 mmol) in 5 mL EtOH and stirred for 20 min. The clear solution was allowed to stand for a few days. The colorless crystals suitable for single-crystal X-ray structure determination were filtered off, washed with EtOH and dried in air. Yield: 75 % (based on $ZnBr_2$). *Anal.* Calc. for $ZnBr_2C_{12}H_{12}N_4O_2$: C, 30.70; H, 2.58; N, 11.93; Zn, 13.93. Found: C, 30.55; H, 2.77; N, 11.77; Zn, 14.34.

IR (ATR, cm^{-1}): 3439(w), 3392(w), 3319(w), 3262(w), 3157(w), 3046(w), 1709(m), 1678(s), 1618(m), 1596(m), 1554(m), 1422(m), 1395(m), 1329(w), 1235(w), 1222(w), 1150(w), 1121(w), 1096(w), 1061(m), 1029(m), 866(m), 855(m), 799(w), 757(s), 708(m), 651(m), 623(m), 593(s), 496(vs), 446(m).

^{13}C NMR (DMSO-d$_6$, δ/ppm): 150.40 (C-2,6), 122.30 (C-3,5), 142.46 (C-4), 166.59 (C-7).

2.2.3. [$Zn(NO_3)_2(H_2O)(isn)_2$] (3)

$Zn(NO_3)_2{\cdot}6H_2O$ (0.30 g, 1 mmol) and isn (0.25 g, 2 mmol) were dissolved in EtOH (15 mL) in a round-bottom flask. The reaction mixture was heated with reflux for 4 h. Hot solution was filtered and left standing on room temperature for a few days. The colorless crystals suitable for single-crystal X-ray structure determination were filtered off, washed with EtOH and dried in air. Yield: 46 % (based on $Zn(NO_3)_2{\cdot}6H_2O$). *Anal.* Calc. for $ZnC_{12}H_{14}N_6O_9$: C, 28.43; H, 2.73; N, 9.47; Zn, 13.93. Found: C, 28.77; H, 2.95; N, 9.56; Zn, 13.93.

IR (ATR, cm^{-1}): 3439-3203(w, br), 3066(w), 1690(m), 1653(m), 1613(w), 1554(w), 1473 (vs), 1419(s), 1336(w), 1283(vs), 1224 (m), 1151(w), 1123(w), 1068(m), 1024(s), 890(w), 855(m), 811(w), 769(m), 629(m), 537(m, br).

^{13}C NMR (DMSO-d$_6$, δ/ppm): 150.63 (C-2,6), 122.94 (C-3,5), 141.91 (C-4), 166.72 (C-7).

2.2.4. [$Zn(CH_3COO)_2(isn)]_2$ (4)

A solution of isn (0.40 g, 3.2 mmol) in 10 mL EtOH was added dropwise to a hot solution of $Zn(CH_3COO)_2$ (0.30 g, 1.6 mmol) in 35 mL EtOH and stirred for 30 min. The clear solution was allowed to stand for a few days. The colorless crystals suitable for single-crystal X-ray structure determination were filtered off, washed with EtOH and dried in air. Yield: 30 % (based on $Zn(CH_3COO)_2$). *Anal.* Calc. for $Zn_2C_{20}H_{24}N_4O_{10}$: C, 39.30; H, 3.96; N, 9.17; Zn, 21.40. Found: C, 38.99; H, 4.11; N, 9.50; Zn, 21.37.

IR (ATR, cm^{-1}): 3388(w), 3195(w), 3099(w), 1699(m), 1597(s), 1567(m), 1425(s, br), 1395(s), 1341(m), 1223(v), 1151(w), 1118(w), 1066(m), 1025(m), 943(w), 865(m), 779(w), 686(m), 646(s), 589(m, br), 499(w), 450(w).

^{13}C NMR (DMSO-d$_6$, δ/ppm): 150.45 (C-2,6), 122.31 (C-3,5), 142.55 (C-4), 166.54 (C-7), 177.55 (COO), 22.91 (CH_3).

2.2.5. [$Zn(isn)_4(H_2O)_2](ClO_4)_2$ (5)

A solution of isn (0.20 g, 1.6 mmol) in 5 mL EtOH was added dropwise to a solution of $Zn(ClO_4)_2{\cdot}6H_2O$ (0.30 g, 0.8 mmol) in 5 mL EtOH and stirred for 30 min. The clear solution was allowed to stand for a few days. The colorless crystals suitable for single-crystal X-ray structure determination were filtered off, washed with EtOH and dried in air. Yield: 45 % (based on $Zn(ClO_4)_2$). *Anal.* Calc. for $ZnCl_2C_{24}H_{28}N_8O_{14}$: C, 36.54; H, 3.58; N, 14.20; Zn, 8.29. Found: C, 35.98; H, 3.84; N, 14.55; Zn, 7.78.

IR (ATR, cm^{-1}): 3466-3201(w, br), 3077(w), 3058(w), 1677(m), 1653(m), 1612(w), 1599(m), 1555(m), 1425(m), 1412(m), 1230(w), 1135(m), 1104(m), 1089(m), 1050(s), 930(w), 853(m), 782(w), 766(m), 723(w), 715(w), 680(m), 616(vs), 552(w), 480(m, br), 441(m).

^{13}C NMR (DMSO-d$_6$, δ/ppm): 150.55 (C-2,6), 122.04 (C-3,5), 142.10 (C-4), 166.80 (C-7).

2.3. X-ray crystallographic analysis

The suitable single crystals of **1**–**5** were selected and mounted onto thin glass fibers. The data collection was carried out on an Oxford Diffraction Xcalibur four-circle kappa geometry diffractometer with Xcalibur Sapphire 3 CCD detector, using graphite monochromated MoKα (λ = 0.71073 Å) radiation at room temperature (296(2) K) and by applying the CrysAlis PRO Software system [34]. The data reduction and cell refinement were performed by the CrysAlis PRO Software system [34]. The structures were solved by SHELXT [35] and refined by SHELXL-2018/3 [36]. The refinement procedure was done by full-matrix least-squares methods based on F^2 values against all reflections. The perchlorate O8 atom in **5** was disordered and had to be refined in two positions, resulting with a site occupancy factor of 0.67(1) (all figures show only one component of the disordered atom, O8A). All the perchlorate Cl–O bond lengths were refined freely. The figures were made with MERCURY (Version 2020.2.0) [37]. The crystallographic data for **1**–**5** are summarized in Tables 1 and 2.

3. Results and discussion

3.1. Synthesis

Compounds **1**–**5** were prepared from ethanol or aqueous solutions by reactions of isn with the corresponding zinc(II) salts using two different

Table 1. The crystallographic data for **1** and **2**.

Compound	**1**	**2**
Formula	$C_{12}H_{12}ZnCl_2N_4O_2$	$C_{12}H_{12}ZnBr_2N_4O_2$
M_r	380.53	469.45
Crystal system, space group	monoclinic, $P2_1/c$ (No. 14)	monoclinic, $P2_1/c$ (No. 14)
a (Å)	5.50104(13)	5.59180(10)
b (Å)	18.0280(4)	18.2062(5)
c (Å)	15.1935(4)	15.2951(4)
β (°)	96.425(2)	94.890(2)
V (Å^3)	1497.32(6)	1551.46(7)
Z	4	4
D_{calc} (g cm^{-3})	1.688	2.010
μ (mm^{-1})	2.005	6.742
R [$I \geq 2\sigma(I)$]	0.0194	0.0224
wR [all data]	0.0534	0.0450

Table 2. The crystallographic data for **3**–**5**.

Compound	**3**	**4**	**5**
Formula	$C_{12}H_{14}ZnN_6O_9$	$C_{20}H_{24}Zn_2N_4O_{10}$	$C_{24}H_{28}ZnCl_2N_8O_{14}$
M_r	451.66	611.17	788.81
Crystal system, space group	monoclinic, $P2_1/c$ (No. 14)	monoclinic, $P2_1/c$ (No. 14)	monoclinic, $C2/c$ (No. 15)
a (Å)	7.4807(3)	13.7945(2)	18.9146(4)
b (Å)	10.6471(4)	11.8202(2)	9.2189(3)
c (Å)	21.5855(8)	14.6283(2)	18.4655(4)
β (°)	95.107(4)	91.8190(10)	92.451(2)
V (Å^3)	1712.41(11)	2384.00(6)	3216.92(14)
Z	4	4	4
D_{calc} (g cm^{-3})	1.752	1.703	1.629
μ (mm^{-1})	1.499	2.075	1.010
R [$I \geq 2\sigma(I)$]	0.0289	0.0215	0.0450
wR [all data]	0.0769	0.0632	0.1299

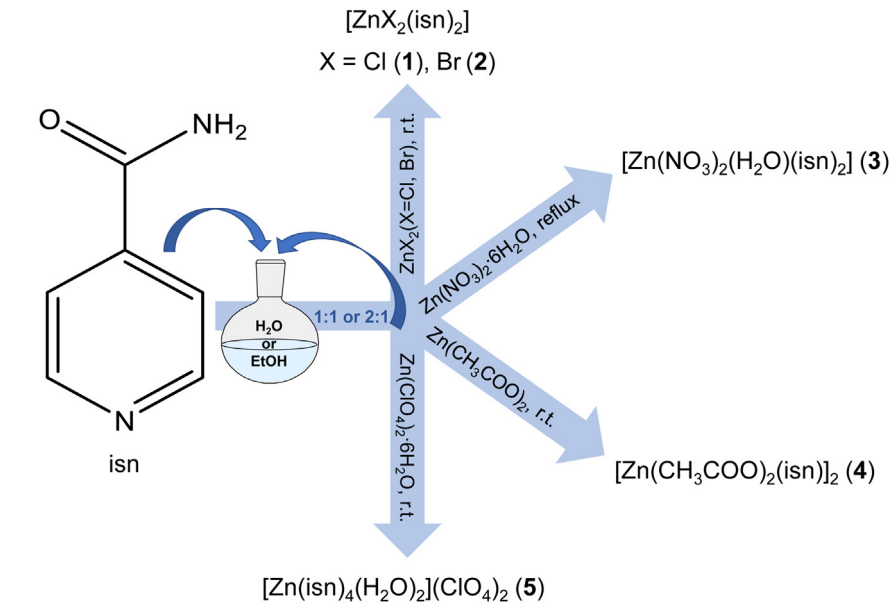

Scheme 2. Preparation of $[ZnCl_2(isn)_2]$ (**1**), $[ZnBr_2(isn)_2]$ (**2**), $[Zn(NO_3)_2(H_2O)(isn)_2]$ (**3**), $[Zn(CH_3COO)_2(isn)]_2$ (**4**) and $[Zn(isn)_4(H_2O)_2](ClO_4)_2$ (**5**) by reactions of pyridine-4-carboxamide (isn) with zinc(II) chloride, zinc(II) bromide, zinc(II) nitrate hexahydrate, zinc(II) acetate and zinc(II) perchlorate hexahydrate, respectively.

ligand-to-metal ratios, 1:1 and 1:2 (Scheme 2). Regardless of the ratio used, the same type of compounds was always obtained. Performing reactions in ethanol solution using 2:1 stoichiometry resulted with faster reactions and higher yields.

We used PXRD to confirm phase purity and bulk composition of compounds **1**–**5** (Figures 1 and S1). The PXRD patterns (bulk sample) of the prepared compounds are consistent with the patterns calculated from the single crystal diffraction data, indicating phase purity of zinc(II) compounds. Purity of prepared compounds was additionally confirmed by the Rietveld refinement (Figures S2-S6). Excellent agreement is observed between experimental and calculated profiles for all compounds (agreement factors: **1** - $R_{wp} = 0.0710$, $R_p = 0.0531$; **2** - $R_{wp} = 0.0564$, $R_p = 0.0437$; **3** - $R_{wp} = 0.0843$, $R_p = 0.0643$; **4** - $R_{wp} = 0.0644$, $R_p = 0.0475$; **5** - $R_{wp} = 0.0892$, $R_p = 0.0689$).

3.2. Crystal structures

The asymmetric units of $[ZnCl_2(isn)_2]$ (**1**) and $[ZnBr_2(isn)_2]$ (**2**) are composed of a zinc(II) ion, two coordinated halide ions (chloride in **1** and bromide in **2**) and two coordinated isonicotinamide molecules (Figure 2a). The overlay of the corresponding molecules of **1** and **2** (Figure 2b) shows the compounds **1** and **2** to be isostructural, which is also supported by the fact both compounds crystallize in the same space group ($P2_1/c$) and with similar unit cell parameters (Table 1). Furthermore, the PXRD traces of **1** and **2** overlap nicely (Figure S1). The zinc(II) ions in **1** and **2** are tetracoordinated, each with two halide ions (Cl1 and Cl2 in **1** and Br1 and Br2 in **2**) and with pyridine N1 and N3 atoms from the isonicotinamide molecules, bound in an *N*-monodentate fashion (Figure 2a, Table S1). The τ_4 values [38] (0.90 for **1** and **2**) indicate the

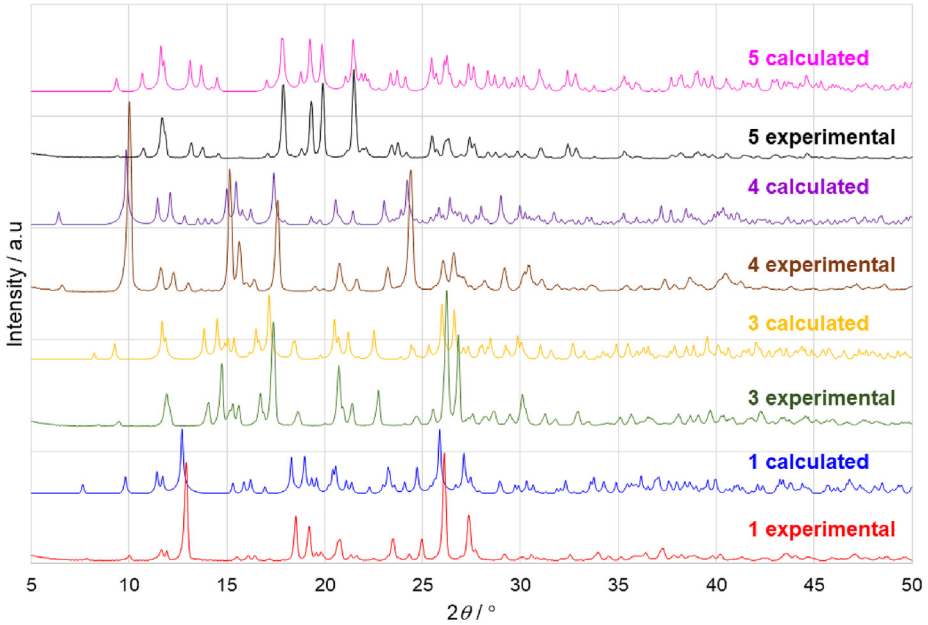

Figure 1. Overlay of experimental and calculated PXRD patterns of **1**, **3**–**5**.

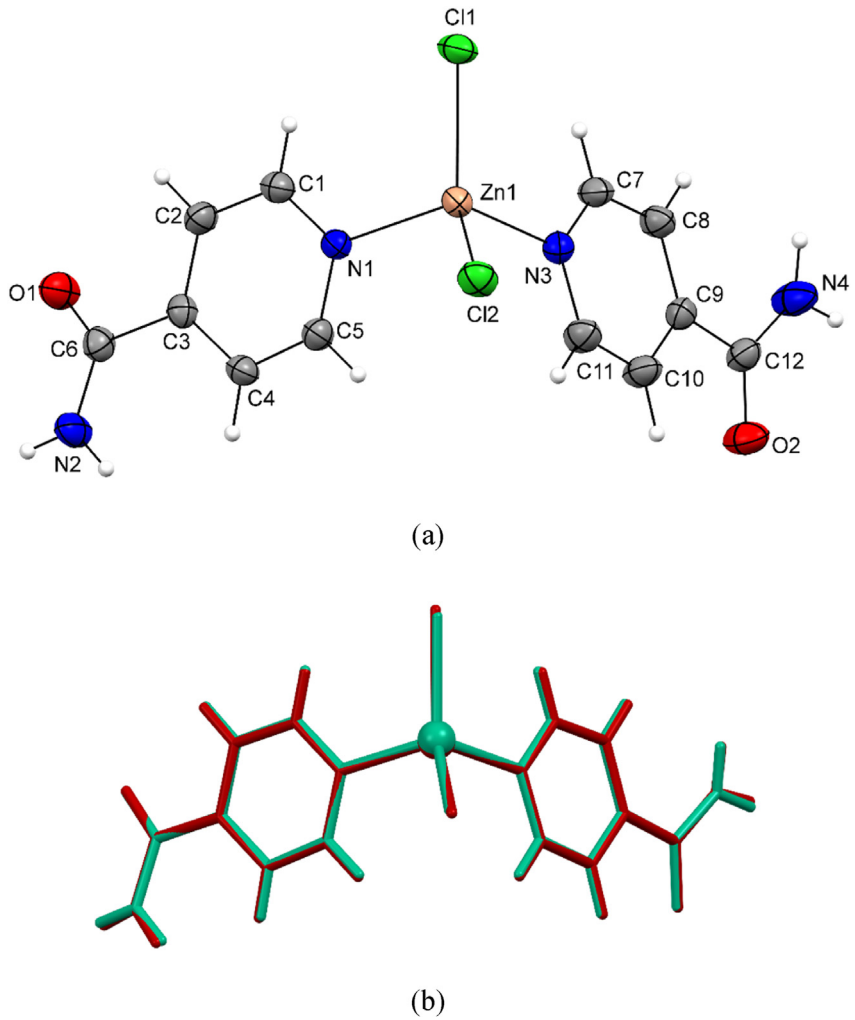

Figure 2. ORTEP-style plot of $[ZnCl_2(isn)_2]$ (**1**) with the atomic numbering scheme of the asymmetric unit. Thermal ellipsoids are drawn at the 40% probability level at 296(2) K and hydrogen atoms are shown as spheres of arbitrary radii (a). Overlay (RMS value of 0.0647 Å) of molecules of $[ZnCl_2(isn)_2]$ (**1**) (green) and $[ZnBr_2(isn)_2]$ (**2**) (brown). The Zn, N, O and halide atoms were chosen for the overlay (b).

tetrahedral zinc(II) coordination environments in both **1** and **2**, also being distorted as can be seen from the bond angles around zinc(II) ions (a range of 104.87(5)°–124.88(2)° in **1** and of 105.33(6)°–123.92(2)° in **2**, Table S1). The analogous (but not isostructural) zinc(II) complexes with isonicotinamide and iodide ions, $[ZnI_2(isn)_2]$ [39], and with pyridine-3-carboxamide (nicotinamide, nia) and chloride or bromide ions, $[ZnCl_2(nia)_2]$ [40] and $[ZnBr_2(nia)_2]$ [41], respectively, are known.

The asymmetric unit of $[Zn(NO_3)_2(H_2O)(isn)_2]$ (**3**) is composed of a zinc(II) ion, two coordinated nitrate ions (one monodentate, the other bidentate), one coordinated water molecule and two coordinated isonicotinamide molecules (Figure 3). The zinc(II) ion in **3** is octahedrally

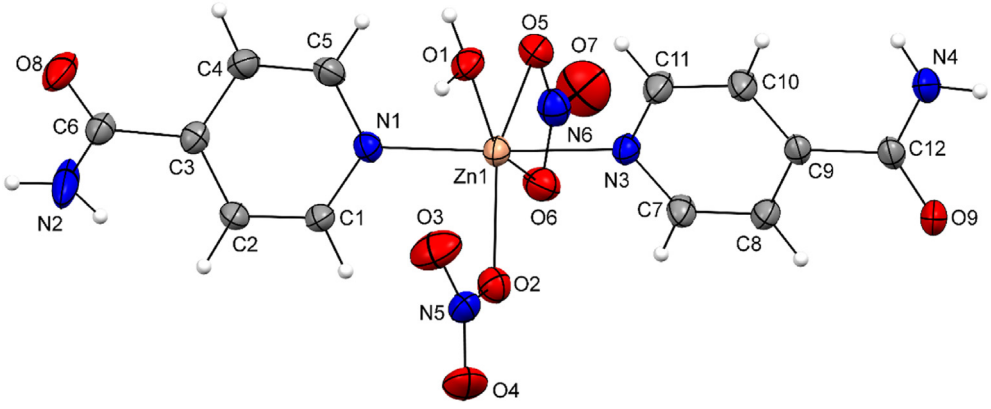

Figure 3. ORTEP-style plot of $[Zn(NO_3)_2(H_2O)(isn)_2]$ (**3**) with the atomic numbering scheme of the asymmetric unit. Thermal ellipsoids are drawn at the 40% probability level at 296(2) K and hydrogen atoms are shown as spheres of arbitrary radii.

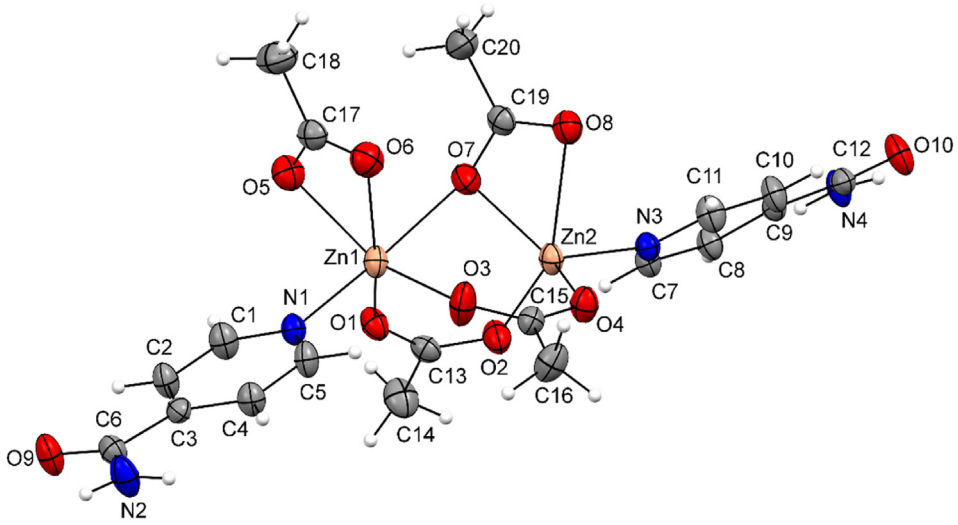

Figure 4. ORTEP-style plot of $[Zn(CH_3COO)_2(isn)]_2$ (**4**) with the atomic numbering scheme of the asymmetric unit. Thermal ellipsoids are drawn at the 40% probability level at 296(2) K and hydrogen atoms are shown as spheres of arbitrary radii.

coordinated with an O2 atom from *O*-monodentate nitrate ion, O5 and O6 atoms from *O,O′*-bidentate nitrate ion and with a water molecule (O1 atom) in the equatorial plane, while pyridine N1 and N3 atoms from *N*-monodentate isonicotinamide molecules are placed in the axial positions (the bond angle N3–Zn1–N1 = 177.05(7)°) of the highly distorted octahedron (Figure 3, Table S2)). This distortion is evident from the bond angles around zinc(II) ion, which are in the range of 139.90(7)°–177.05(7)° for the *trans* pairs of the coordinated atoms and of 56.43(7)°–124.62(7)° for the *cis* pairs (Table S2). The reason for such a high distortion of the octahedron is probably the *O,O′*-bidentate binding of the nitrate ion and the formation of three-membered chelate ring Zn1/O5/O6, with a very small bite angle O6–Zn1–O5 (56.43(7)°) (Table S2).

The asymmetric unit of $[Zn(CH_3COO)_2(isn)]_2$ (**4**) is composed of two zinc(II) ions, four coordinated acetate ions and two coordinated isonicotinamide molecules (Figure 4); two crystallographically independent zinc(II) ions being bridged with three acetate ions into a dimer (Zn···Zn separation of 3.2884(4) Å) of **4**. Those four acetate ions are bound in three different coordination modes: two of them are bridging (each O atom (O1, O2, O3 and O4) is bound to a separate Zn(II) ion), the third is chelating (both O atoms (O5 and O6) are bound to the same Zn(II) ion) and the fourth is both chelating and bridging (one of the O atoms (O7) is bound to both Zn(II) ions). One of the zinc(II) ions in **4** (Zn1) is octahedrally coordinated with O1 and O3 atoms (each from separate bridging acetate ions) and with O5 and O6 atoms from the chelating acetate in the equatorial plane, while pyridine N1 atom from *N*-monodentate isonicotinamide molecule and O7 atom (from chelating and bridging acetate ion) are placed in the axial positions (the bond angle N1–Zn1–O7 = 175.15(5)°) of the highly distorted octahedron (Figure 4, Table S2). The other zinc(II) ion (Zn2) is pentacoordinated with O2 and O4 atoms from two separate bridging acetate ions, O7 and O8 atoms from the chelating and bridging acetate ion and with a pyridine N3 atom from an *N*-monodentate isonicotinamide molecule (Figure 4, Table S2). The τ value [42] of 0.46 suggests that the zinc(II) coordination environment around Zn2 ion can be best described as an intermediate between a square pyramid and a trigonal bipyramid. Both zinc(II) coordination environments are highly distorted, as can be seen from the bond angles around the octahedral Zn1 ion (a range of 153.15(7)°–175.15(5)° for the *trans* pairs of the coordinated atoms and of 59.69(6)°–105.64(7)° for the *cis* pairs) and around the pentacoordinated Zn2 ion (a range of 57.65(5)°–150.85(6)°, Table S2). Such high distortion of the coordination environments are probably caused by the *O,O′*-bidentate binding of the acetate ions, leading to the formation of three-membered chelate rings (Zn1/O5/O6 and Zn2/O7/O8), with very small bite angles O6–Zn1–O5 (59.69(6)°) and O7–Zn2–O8 (57.65(5)°) (Table S2). The similar zinc(II) complex with nicotinamide and acetate ions, $[Zn(CH_3COO)_2(nia)]_2{\cdot}2H_2O$ [43], is known. In contrast to **4**, all four acetate ions are coordinated to zinc(II) ions in the same bridging coordination mode – each carboxylate O atom being bound to a separate zinc(II) ion. Consequently, both zinc(II) ions are pentacoordinated (a square pyramid), as opposed to octahedral and pentacoordinated (an intermediate between a square pyramid and a trigonal bipyramid) zinc(II) ions in **4**. Another difference is presence of lattice water molecules, being hydrogen-bonded to nicotinamide O atoms, in the crystal structure of $[Zn(CH_3COO)_2(nia)]_2{\cdot}2H_2O$ [43].

The asymmetric unit of $[Zn(isn)_4(H_2O)_2](ClO_4)_2$ (**5**) is composed of a zinc(II) ion (lying on a two-fold rotation axis), two coordinated water molecules, two coordinated isonicotinamide molecules and an uncoordinated perchlorate ion (Figure 5). The zinc(II) ion in **5** is octahedrally

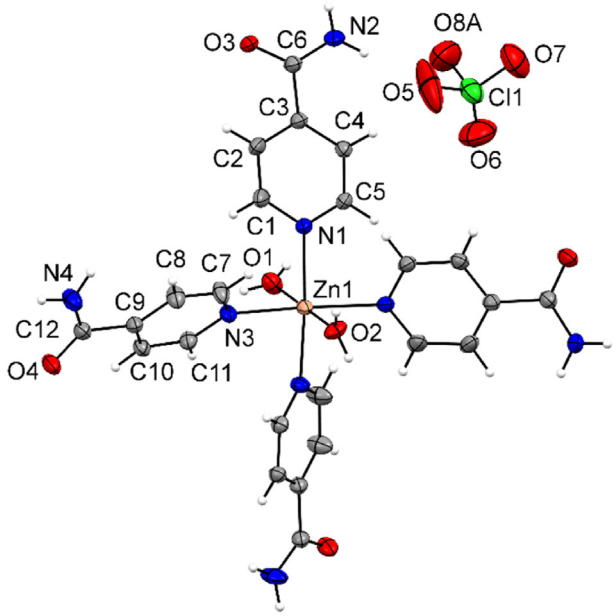

Figure 5. ORTEP-style plot of $[Zn(isn)_4(H_2O)_2](ClO_4)_2$ (**5**) with the atomic numbering scheme of the asymmetric unit. Thermal ellipsoids are drawn at the 40% probability level at 296(2) K and hydrogen atoms are shown as spheres of arbitrary radii. The O8B component of the disordered perchlorate O8 atom is not shown.

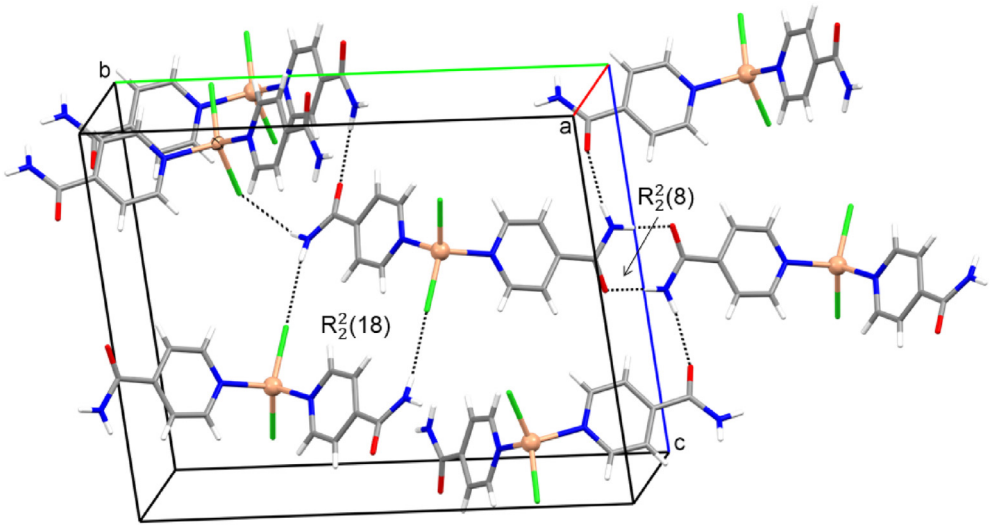

Figure 6. The hydrogen-bonded ring motifs (shown by dotted lines) found within the hydrogen-bonded framework of $[ZnCl_2(isn)_2]$ (**1**) e. g. the dimeric amide-amide $R_2^2(8)$ motif and dimeric $R_2^2(18)$ motif.

coordinated with pyridine N1, N3, $N1^i$ and $N3^i$ atoms (symmetry code (i): $-x + 1$, y, $-z + 1/2$) from four *N*-monodentate isonicotinamide molecules in the equatorial plane and with two water molecules (O1 and O2 atoms) in the axial positions (the bond angle O2–Zn1–O1 = 180°, Table S2). The zinc(II) coordination environment is only slightly distorted, as evident from the bond angles around zinc(II) ion (a range of 170.7(2)°–180° for the *trans* pairs of the coordinated atoms and of 85.34(7)°–94.66(7)° for the *cis* pairs (Table S2)). The Zn–N bond lengths in **1**–**5** are comparable to those seen in the related zinc(II) compounds containing coordinated isonicotinamide via its pyridine N atom [39, 44], whilst the Zn–X (X = Cl, Br) and Zn–O (O atom from nitrate or acetate ions) bond lengths are found within the expected range [45].

There are strong intermolecular N–H···O hydrogen bonds observed in all the structures of **1**–**5**, while the O–H···O hydrogen bonds are present only in the structures of **3** and **5** and the N–H···Cl and N–H···Br hydrogen bonds only in the respective structures of **1** and **2** (Table S3). These hydrogen bonds are responsible for assembling the respective coordination compound molecules (including perchlorate ions in **5**) into complex hydrogen-bonded frameworks of **1**–**5**. The centrosymmetric dimeric amide-amide $R_2^2(8)$ motif was found in the hydrogen-bonded frameworks of **1**–**4**, as expected (Figures 6, 7, and 8). However, the amide O atoms are not the sole proton acceptors in either of these structures and always compete with other possible proton acceptors for the amide group protons, which may lead to the possible disruption of the amide-amide $R_2^2(8)$ motif and the formation of different hydrogen-bonded ring motifs. Indeed, the coordinated chloride (in **1**) or bromide (in **2**) ions also act as proton acceptors, leading to the formation of centrosymmetric dimeric $R_2^2(18)$ motif in the hydrogen-bonded frameworks of **1** and **2** (Figure 6). Furthermore, the nitrate and acetate O atoms in the structures of **3** and **4**, respectively, act as proton acceptors as well and form the additional dimeric $R_2^2(18)$ and $R_2^2(20)$ motifs, the trimeric $R_3^2(20)$ motif (in **3**, Figure 7) and the dimeric $R_2^2(22)$ and tetrameric $R_4^4(22)$ motifs (in **4**, Figure 8). Furthermore, the presence of the perchlorate O atom as a proton acceptor in the hydrogen-bonded framework of **5** leads to the disruption of the amide-amide $R_2^2(8)$ motif and to the formation of different motifs in which both amide groups and coordinated water molecules participate e. g. the dimeric $R_2^2(18)$ and $R_2^2(28)$ motifs and tetrameric $R_4^3(12)$ motif (Figure 9).

3.3. Spectroscopic studies

The recorded IR spectra of coordination compounds **1**–**5** (Figures S7 and S8) are in a good agreement with their crystal structures. Absorption

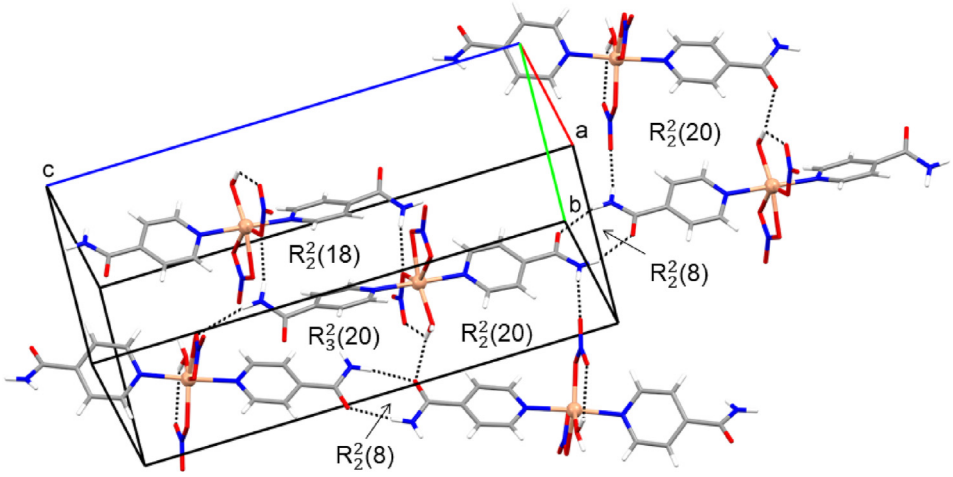

Figure 7. The hydrogen-bonded ring motifs (shown by dotted lines) found within the hydrogen-bonded framework of $[Zn(NO_3)_2(H_2O)(isn)_2]$ (**3**) e. g. the dimeric amide-amide $R_2^2(8)$ motif, dimeric $R_2^2(18)$ and $R_2^2(20)$ motifs and the trimeric $R_3^2(20)$ motif.

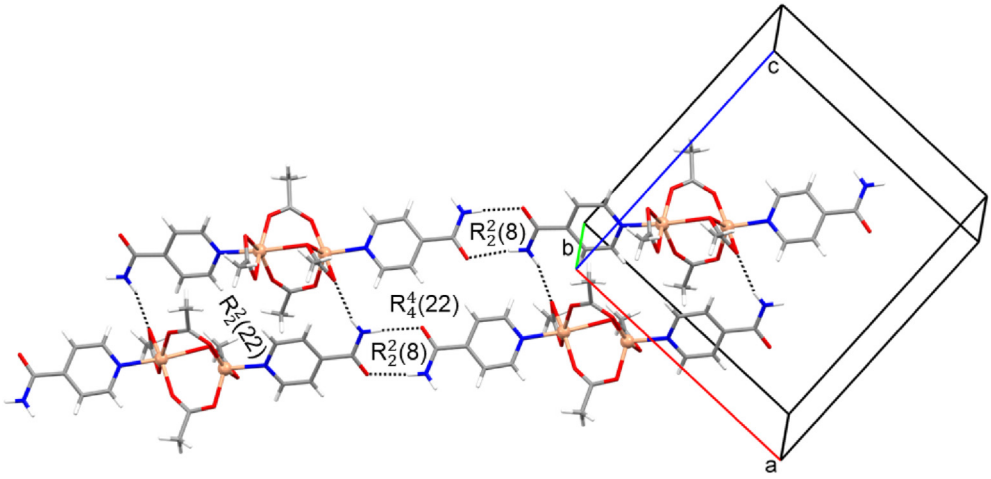

Figure 8. The hydrogen-bonded ring motifs (shown by dotted lines) found within the hydrogen-bonded framework of $[Zn(CH_3COO)_2(isn)]_2$ (**4**) e. g. the dimeric amide-amide $R_2^2(8)$ motif, dimeric $R_2^2(22)$ and tetrameric $R_4^4(22)$ motifs.

bands observed in the spectra of compounds **1**, **2** and **4** in the 3440-3380 cm^{-1} and 3320-3260 cm^{-1} region can be attributed to antisymmetric stretching vibrations of the amide group. Symmetric stretching vibrations of the amide group are in the spectra of the compounds **1**, **2** and **4** observed in the 3195-3100 cm^{-1} region [39, 46, 47]. Broadening of the amide stretching vibrations in the IR spectra of **3** and **5** can be attributed to the overlapping with O–H stretching vibrations of the coordinated water molecules [39]. Broad bands, due to the extensive hydrogen bonding, are observed in the 3470−3200 cm^{-1} region in the IR spectra of **3** and **5**. The characteristic ν(C=O) bands of amide group are observed at 1717 cm^{-1}, 1678 cm^{-1} (**1**), 1709 cm^{-1}, 1678 cm^{-1} (**2**), 1690 cm^{-1} (**3**), 1699 cm^{-1} (**4**) and 1677 cm^{-1} (**5**), due to the existence of uncoordinated amide group [39, 47]. The blue shift of the absorption band attributed to the ring breathing vibrational mode at 1061 cm^{-1} (**1**), 1061 cm^{-1} (**2**), 1068 cm^{-1} (**3**), 1066 cm^{-1} (**4**) and 1089 cm^{-1} (**5**), when compared to band of the uncoordinated ligand (994 cm^{-1}), suggests coordination of the isn ligand via pyridine N atom [39, 46, 48]. Furthermore, IR spectra of compounds **3**–**5** exhibit broad bands related to the vibrations of oxoanions [49]. IR spectrum of the nitrate compound **3** displays three strong bands at 1473, 1283 and 1024 cm^{-1} due to the coordinated nitrate ions. Two broad bands in the region 1650-1500 cm^{-1} (centered at 1597 and 1567 cm^{-1}) and region 1450-1300 cm^{-1} (centered at 1425 and 1395 cm^{-1}) in the IR spectrum of the **4** correspond to the antisymmetric and symmetric stretching vibrations of the acetate ions, respectively [2, 49]. Broadening and splitting of the aforementioned bands is connected with three different coordination modes of acetate ligand. The broad intensive band in the IR spectrum of **5** centered around 1050 cm^{-1} and weak band at 930 cm^{-1} are related to the vibrations of uncoordinated perchlorate ion [49].

The ^{13}C NMR data for compounds **1**–**5** are given in the Experimental section and NMR spectra of the isn and zinc compounds available in SI (Figures S9-S14). The numeration of the atoms is consistent with IUPAC nomenclature (Scheme 3). Almost identical ^{13}C NMR spectra of isn [150.65 (C-2,6), 121.87 (C-3,5), 141.74 (C-4), 166.87 (C-7)] and **3**

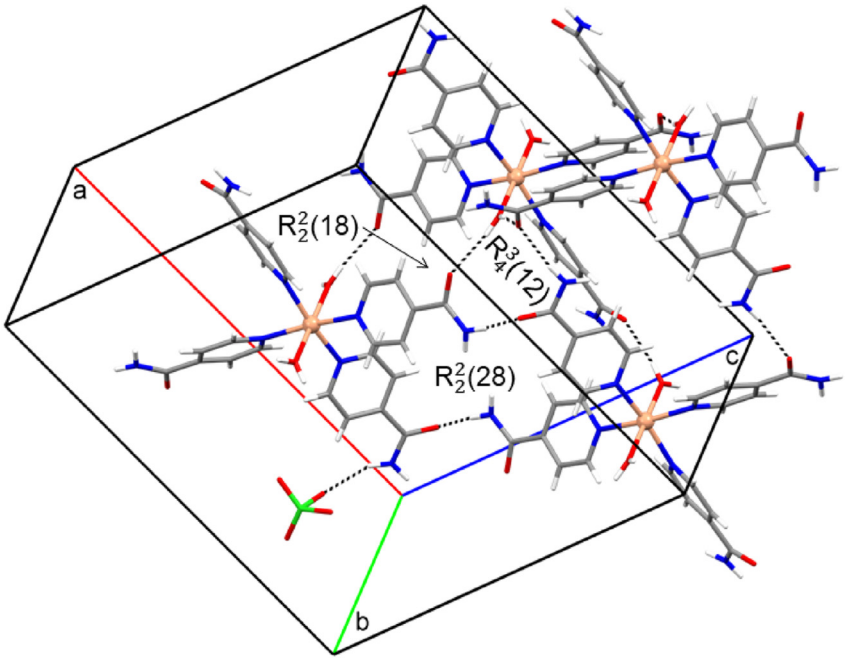

Figure 9. The hydrogen-bonded ring motifs (shown by dotted lines) found within the hydrogen-bonded framework of $[Zn(isn)_4(H_2O)_2](ClO_4)_2$ (**5**) e. g. the dimeric $R_2^2(18)$ and $R_2^2(28)$ motifs and tetrameric $R_4^3(12)$ motif.

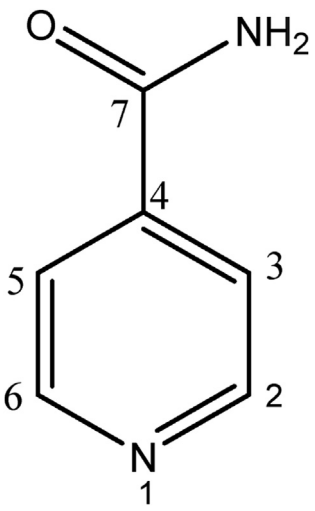

Scheme 3. Numeration of the atoms in ina.

suggests decomposition of **3** in DMSO solution. The greatest change is observed for the chemical shift of the C-4 atom (deshielding effect, 0.36–0.81 ppm) in the ^{13}C NMR spectra of the **1**, **2**, **4** and **5** upon complexation with zinc(II). The largest shielding effect (0.07–0.33 ppm) was observed on the carboxylic carbon atom (C-7). Although small, such complexation effects observed for compounds **1**, **2**, **4** and **5** are consistent with solid state structure of the mentioned compounds.

3.4. Thermal studies

The thermal stability of the compounds was studied in flowing nitrogen by TGA and DSC methods (Figures S15-S18). Similar thermal behavior is observed for anhydrous complexes **1**, **2** and **4** while aqua compounds display more complex thermal degradation. Continuous thermal degradation of the compounds **1**, **2** and **4** starts at 228 (**1**), 237 (**2**) and 183 °C (**4**). Total mass losses of 80.84 % (**1**), 93.04 % (**2**) and 71.50 % (**4**) were observed at 600 °C. Thermal degradation is characterized with two (**1**, **2**) and four (**4**) endothermic signals on the DSC curves: 265 and 311 °C, 272 and 346 °C and 223, 259, 268 and 346 °C, respectively. First thermal event is characterized with an intense signal attributed to the melting of the compounds followed by an instantaneous thermal degradation. Thermal decomposition of **3** and **5** starts with elimination of water molecule. First step on TGA curve of **3** is connected with a mass loss of 4.24% from 105 °C to 181 °C, which corresponds to the elimination of one water molecule (calc. 3.99%). A broad endothermic signal with minima at 113 and 122 °C is observed on the DSC curve due to the elimination of one water molecule. Melting of the anhydrous compound followed by partial thermal decomposition is characterized with four signals on the DSC curve: endothermic at 186 °C and broad exothermic signals with maxima at 290, 302 and 335 °C. Similar decomposition pattern is observed for compound **5**. Mass loss of 4.15 % (calc. 4.56 %) in the range of 48–173 °C, observed at the TGA curve of **5**, corresponds to the elimination of two water molecules. The DSC curve reveals corresponding broad endothermic signals at 78 and 121 °C. Intensive broad exothermic signal with maxima at 364 and 372 °C is most likely related to a thermal decomposition of perchlorate anions. Total mass losses of 77.99 % (**3**) and 70.68 % (**5**) were observed at 600 °C.

4. Conclusion

The zinc(II) coordination compounds with isonicotinamide and various anions (halide ions, perchlorate, nitrate, acetate) have been prepared. It was possible to tune the coordination environment of zinc(II) by selecting the said anions. The coordination environment of zinc(II) was found to be tetrahedral (low coordination number, as expected) in the compounds containing small halide anions (chloride, bromide), **1** and **2**. However, zinc(II) coordination environment was enlarged to the octahedral in the presence of the nitrate ions, acting as both monodentate and bidentate ligands, in **3**. Moreover, the acetate ions exhibit their full bridging and chelating potential, leading to the formation of a zinc(II) dimer in **4**. The coordination environments of both zinc(II) ions within this dimer of **4** were also enlarged in the comparison with **1** and **2**, but similar to **3**; one zinc(II) being octahedrally coordinated and the other being pentacoordinated (best described as an intermediate between a square pyramid and a trigonal bipyramid). Despite of a perchlorate anion coordination potential, it was not found to be coordinated to zinc(II) ion in **5**, most probably due to its bulkiness. Nevertheless, the uncoordinated perchlorate anion didn't prevent zinc(II) ion to reach its higher coordination environment (octahedron) by binding four *N*-monodentate isonicotinamide ligands and two water molecules. Indeed, isonicotinamide ligand acted as an *N*-monodentate ligand in all the prepared zinc(II) compounds, as we hoped it would, leaving the corresponding amide groups uncoordinated.

The anticipated supramolecular amide-amide homosynthon $R_2^2(8)$ was found to be preserved in the hydrogen-bonded frameworks of **1**-**4**, which suggests that the presence of halide ions, nitrate and acetate do not disrupt the formation of this homosynthon, in spite of the simultaneous formation of the additional, rival hydrogen-bonded ring motifs, in which the amide groups also participate. These results are completely in accordance with the literature findings; the said homosynthon being also preserved in the hydrogen-bonded frameworks of the similar metal(I,II)-isonicotinamide compounds containing halide, nitrate or acetate ions (metals: silver(I), copper(II), cobalt(II), strontium(II)) [3, 5, 8, 20, 50, 51, 52, 53]. Finally, the amide-amide $R_2^2(8)$ homosynthon was not found at all in the hydrogen-bonded framework of **5**. Thus, the perchlorate anion is the only anion in this study which is capable of a complete disruption of the said homosynthon, most probably due to its bulkiness in comparison with the other studied anions. Again, these findings are consistent with the literature – the said homosynthon was never found in the hydrogen-bonded frameworks of the similar metal(I,II)-isonicotinamide compounds containing perchlorate ions (metals: silver(I), copper(II), nickel(II)) [9, 16, 54]. Therefore, the role of the particular anion in the said homosynthon preservation/disruption can be predicted with a relative certainty – halide, nitrate and acetate ions lead to the preservation of the homosynthon, whilst perchlorate ions cause its disruption.

Declarations

Author contribution statement

Željka Soldin: Conceived and designed the experiments; Performed the experiments; Analyzed and interpreted the data; Wrote the paper.

Boris-Marko Kukovec: Analyzed and interpreted the data; Wrote the paper.

Tamara Debač, Marijana Đaković: Performed the experiments; Analyzed and interpreted the data.

Zora Popović: Analyzed and interpreted the data; Contributed reagents, materials, analysis tools or data.

Funding statement

This work was supported by University of Zagreb, Zagreb, Croatia (Grant No. 118120281106), the Ministry of Science, Education and Sports of the Republic of Croatia (Grant No. 119-1193079-1332) and the European Regional Development Fund (infrastructural project CIuK, Grant No. KK.01.1.1.02.0016).

Data availability statement

Data included in article/supplementary material/referenced in article.

Declaration of interests statement

The authors declare the following conflict of interest: B.-M. Kukovec is an Associate Editor of Heliyon (section: Chemistry).

Additional information

Deposition numbers 2158537-2158541 for **1**–**5** contain the supplementary crystallographic data for this paper. These data are provided free of charge by the joint Cambridge Crystallographic Data Centre and Fachinformationszentrum Karlsruhe Access Structures service at www.ccdc.cam.ac.uk/structures.

Supplementary content related to this article has been published online at https://doi.org/10.1016/j.heliyon.2022.e09943.

References

[1] G. Yang, H.-G. Zhu, B.-H. Liang, X.-M. Chen, Syntheses and crystal structures of four metal–organic co-ordination networks constructed from cadmium(II) thiocyanate and nicotinic acid derivatives with hydrogen bonds, J. Chem. Soc. Dalton Trans. (2001) 580–585.

[2] B. Dojer, A. Pevec, F. Belaj, Z. Jagličić, M. Kristl, M. Drofenik, Structural and magnetic properties of cobalt(II) complexes with pyridinecarboxamide ligands, J. Mol. Struct. 1076 (2014) 713–718.

[3] C.B. Aakeröy, A.M. Beatty, J. Desper, M. O'Shea, J. Valdés-Martínez, Directed assembly of dinuclear and mononuclear copper(II)-carboxylates into infinite 1-D motifs using isonicotinamide as a high-yielding supramolecular reagent, Dalton Trans (2003) 3956–3962.

[4] C.B. Aakeröy, A.M. Beatty, D.S. Leinen, K.R. Lorimer, Deliberate combination of coordination polymers and hydrogen bonds in a supramolecular design strategy for inorganic/organic hybrid networks, Chem. Commun. (2000) 935–936.

[5] N. Hearne, M.M. Turnbull, C.P. Landee, E.M. van der Merwea, M. Rademeyer, Halide-bi-bridged polymers of amide substituted pyridines and pyrazines: polymorphism, structures, thermal stability and magnetism, CrystEngComm 21 (2019) 1910–1927.

[6] J.-P. Zhang, Y.-Y. Lin, X.-C. Huang, X.-M. Chen, Copper(I) 1,2,4-triazolates and related complexes: studies of the solvothermal ligand reactions, network topologies, and photoluminescence properties, J. Am. Chem. Soc. 127 (2005) 5495–5506.

[7] F. Sánchez-Férez, D. Ejarque, T. Calvet, M. Font-Bardia, J. Pons, Isonicotinamide-based compounds: from cocrystal to polymer, Molecules 24 (2019) 4169.

[8] S.M. Fellows, T.J. Prior, Polymorphism and solid−gas/solid−solid reactions of isonicotinic acid, isonicotinamide, and nicotinamide copper chloride compounds, Cryst. Growth Des. 17 (2017) 106–116.

[9] M. Đaković, Z. Popović, Uncommon isonicotinamide supramolecular synthons in copper(II) complexes directed by nitrate and perchlorate anions, Acta Crystallogr. C65 (2009) m361–m366.

[10] A. Angeloni, A.G. Orpen, Control of hydrogen bond network dimensionality in tetrachloroplatinate salts, Chem. Commun. (2001) 343–344.

[11] A. Mishra, R. Gupta, Supramolecular architectures with pyridine-amide based ligands: discrete molecular assemblies and their applications, Dalton Trans 43 (2014) 7668–7682.

[12] A. Mukherjee, Building upon supramolecular synthons: some aspects of crystal engineering, Cryst. Growth Des. 15 (2015) 3076–3085.

[13] C.B. Aakeröy, B.M.T. Scott, J. Desper, How robust is the hydrogen-bonded amide 'ladder' motif? New J. Chem. 31 (2007) 2044–2051.

[14] J.K. Bera, T.-T. Vo, R.A. Walton, K.R. Dunbar, Hydrogen-bonding as a tool for building one-dimensional structures based on dimetal building blocks, Polyhedron 22 (2003) 3009–3014.

[15] M. Đaković, Z. Jagličić, B. Kozlevčar, Z. Popović, Association of copper(II) isonicotinamide moieties via different anionic bridging ligands: two paths of ferromagnetic interaction in the azide coordination compound, Polyhedron 29 (2010) 1910–1917.

[16] C.B. Aakeröy, A.M. Beatty, D.S. Leinen, A versatile route to porous solids: organic-inorganic hybrid materials assembled through hydrogen bonds, Angew. Chem. Int. Ed. 28 (1999) 1815–1819.

[17] M.M. Wicht, L.R. Nassimbeni, N.B. Báthori, Werner clathrates with enhanced hydrogen bonding functionality, Polyhedron 163 (2019) 7–19.

[18] R. Seetharaj, P.V. Vandana, P. Arya, S. Mathew, Dependence of solvents, pH, molar ratio and temperature in tuning metal organic framework architecture, Arab. J. Chem. 12 (2019) 295–315.

[19] C.-P. Li, M. Du, Role of solvents in coordination supramolecular systems, Chem. Commun. 47 (2011) 5958–5972.

[20] F. Sánchez-Féreza, L. Bayés, M. Font-Bardiac, J. Pons, Solvent dependent formation of Cu(II) complexes based on isonicotinamide, Inorg. Chim. Acta. 494 (2019) 112–122.

[21] J. Zhao, D. Yang, X.-J. Yang, B. Wu, Anion coordination chemistry: from recognition to supramolecular assembly, Coord. Chem. Rev. 378 (2019) 415–444.

[22] A. Rajput, R. Mukherjee, Coordination chemistry with pyridine/pyrazine amide ligands. Some noteworthy results, Coord. Chem. Rev. 257 (2013) 350–368.

[23] M. Đaković, J. Jaźwiński, Z. Popović, Impact of coordinated pseudohalide ions and picolinamide on supramolecular synthons in selected zinc and cadmium complexes, Acta Chim. Slov. 62 (2015) 328–336.

[24] Z. Nezhadali Baghan, A. Salimi, H. Eshtiagh-Hosseinia, A.G. Olive, Hydrogen-bonded 3D network of d^{10}-metal halide coordination polymer containing N-(3-pyridinyl) nicotinamide: influence of ligand conformation, halide anions and solvent, CrystEngComm 21 (2019) 2691–2701.

[25] K.A. McCall, C.-C. Huang, C.A. Fierke, Function and mechanism of zinc metalloenzymes, J. Nutr. 130 (2000) 1437S–1446S.

[26] L. Sreenivas Reddy, A. Nangia, V.M. Lynch, Phenyl-perfluorophenyl synthon mediated cocrystallization of carboxylic acids and amides, Cryst. Growth Des. 4 (2004) 89–94.

[27] M.C. Etter, Hydrogen bonds as design elements in organic chemistry, J. Phys. Chem. 95 (1991) 4601–4610.

[28] D. Markad, S.K. Mandal, An exploration into the amide–pseudo amide hydrogen bonding synthon between a new coformer with two primary amide groups and theophylline, CrystEngComm 19 (2017) 7112–7124.

[29] C.B. Aakeröy, B.M.T. Scott, M.M. Smith, J.F. Urbina, J. Desper, Establishing amide · · · amide reliability and synthon transferability in the supramolecular assembly of metal-containing one-dimensional architectures, Inorg. Chem. 48 (2009) 4052–4061.

[30] S. Tothadi, G.R. Desiraju, Unusual co-crystal of isonicotinamide: the structural landscape in crystal engineering, Phil. Trans. R. Soc. A 370 (2012) 2900–2915.

[31] G.B. Simões, P.V.S. Badolato, M.D. Ignácio, E.C. Cerqueira, Determination of zinc oxide in pharmaceutical preparations by EDTA titration: a practical class for a quantitative analysis course, J. Chem. Educ. 97 (2020) 522–527.

[32] D.C. Harris, Quantitative Chemical Analysis, seventh ed., W. H. Freeman, New York, 2007, pp. 238–241.

[33] A. Coelho, Topas Academic V5, 2013.

[34] P.R.O. CrysAlis, Agilent Technologies Ltd, Yarnton, Oxfordshire, England, 2010.

[35] G.M. Sheldrick, *SHELXT* - integrated space-group and crystal-structure determination, Acta Crystallogr. A71 (2015) 3–8.

[36] G.M. Sheldrick, Crystal structure refinement with *SHELXL*, Acta Crystallogr. C71 (2015) 3–8.

[37] C.F. Macrae, I. Sovago, S.J. Cottrell, P.T.A. Galek, P. McCabe, E. Pidcock, M. Platings, G.P. Shields, J.S. Stevens, M. Towler, P.A. Wood, *Mercury 4.0*: from visualization to analysis, design and prediction, J. Appl. Crystallogr. 53 (2020) 226–235.

[38] L. Yang, D.R. Powell, R.H. Houser, Structural variation in copper(I) complexes with pyridylmethylamide ligands: structural analysis with a new four-coordinate geometry index, τ_4, Dalton Trans (2007) 955–964.

[39] H. Paşaoğlu, S. Güven, Z. Heren, O. Büyükgüngör, Synthesis, spectroscopic and structural investigation of ZnI_2(nicotinamide)$_2$, ZnI_2(isonicotinamide)$_2$ and $[Zn(H_2O)_2(picolinamide)_2]I_2$, J. Mol. Struct. 794 (2006) 270–276.

[40] S. İde, A. Ataç, Ş. Yurdakul, Structural features of dibromobis(nicotinamide)zinc(II) complex, J. Mol. Struct. 605 (2002) 103–107.

[41] E. Şahin, S. İde, A. Ataç, Ş. Yurdakul, Structural features of dibromobis(nicotinamide)zinc(II) complex, J. Mol. Struct. 616 (2002) 253–258.

[42] A.W. Addison, T. Nageswara Rao, J. Reedijk, J. van Rijn, G.C. Verschoor, Synthesis, structure, and spectroscopic properties of copper(II) compounds containing nitrogen–sulphur donor ligands; the crystal and molecular structure of aqua[1,7-bis(N-methylbenzimidazol-2′-yl)-2,6-dithiaheptane]copper(II) perchlorate, J. Chem. Soc. Dalton Trans. (1984) 1349–1356.

[43] D. Chakrabarty, H. Nagase, M. Kamijo, T. Endo, H. Ueda, Crystal Structure of Tetrakis[μ-(acetato-O:O′)]bisnicotinamide-N1-zinc(II)] dihydrate, Anal. Sci. 21 (2005) x167–x168.

[44] T. Neumann, I. Jess, C. Näther, Crystal structure of tetrakis(isonicotinamide-κN) bis(thiocyanato-κN)cobalt(II)–isonicotinamide–ethanol (1/2/1), Acta Crystallogr. E72 (2016) 1077–1080.

[45] C.R. Groom, I.J. Bruno, M.P. Lightfoot, S.C. Ward, The Cambridge structural database, Acta Crystallogr. B72 (2016) 171–179.

[46] O. Treu Filho, J.C. Pinheiro, E.B. da Costa, R.T. Kondo, R.A. de Souza, V.M. Nogueira, A.E. Mauro, Theoretical and experimental study of the infrared spectrum of isonicotinamide, J. Mol. Struct. Theochem. 763 (2006) 175–179.

[47] Ş. Yurdakul, A. Ataç, E. Şahin, S. İde, Synthesis, spectroscopic and structural studies on metal halide complexes of isonicotinamide, Vib. Spectrosc. 31 (2003) 41–49.

[48] R.A. de Souza, A.E. Mauro, A.V.G. Netto, G.A. da Cunha, E.T. de Almeida, Synthesis, characterization, and thermal behavior of palladium(II) coordination compounds containing isonicotinamide, J. Therm. Anal. Calorim. 106 (2011) 375–378.

[49] K. Nakamoto, Infrared and Raman Spectra of Inorganic and Coordination Compounds: Part B: Applications in Coordination, Organometallic, and Bioinorganic Chemistry, sixth ed., John Wiley & Sons, Inc., Hoboken, New Jersey, 2009.

[50] T. Dorn, K.M. Fromm, C. Janiak, $[Ag(isonicotinamide)_2NO_3]_2$ – a stable form of silver nitrate, Aust. J. Chem. 59 (2006) 22–25.

[51] M.A.M. Abu-Youssef, R. Dey, Y. Gohar, A.A. Massoud, L. Öhrström, V. Langer, Synthesis and structure of silver complexes with nicotinate-type ligands having antibacterial activities against clinically isolated antibiotic resistant Pathogens, Inorg. Chem. 46 (2007) 5893–5903.

[52] J. Xue, X. Hua, L. Yang, W. Li, Y. Xu, G. Zhao, G. Zhang, L. Liu, K. Liu, J. Chen, J. Wu, Cobalt(II) and strontium(II) complexes of three isomers, nicotinamide, isonicotinamide and picolinamide, J. Mol. Struct. 1059 (2014) 108–117.

[53] M. Perec, R. Baggio, Di-μ-acetato-bis[(acetato-κ^2O,O')bis-(isonicotinamide-κN) copper(II)], Acta Crystallogr. E66 (2010) m275–m276.

[54] C.B. Aakeröy, A.M. Beatty, B.A. Helfrich, Two-fold interpenetration of 3-D nets assembled via three-co-ordinate silver(I) ions and amide–amide hydrogen bonds, J. Chem. Soc. Dalton Trans. (1998) 1943–1945.